PNAS RESEARCH ARTICLE | IMMUNOLOGY AND INFLAMMATION OPEN ACCESS

Expression of the monocarboxylate transporter MCT1 is required for virus-specific mouse CD8$^+$ T cell memory development

Stefania D'Aria[a,1], Céline Maquet[b,1], Shuang Li[a,1], Suveera Dhup[c], Anouk Lepez[d], Arnaud Kohler[a], Vincent F. Van Hée[c], Rajesh K. Dadhich[c], Marine Frenière[a], Fabienne Andris[d], Ivan Nemazanyy[e], Pierre Sonveaux[c,f,2], Bénédicte Machiels[b,2], Laurent Gillet[b,2], and Michel Y. Braun[a,2,3]

Edited by Rafi Ahmed, Emory University, Atlanta, GA; received May 4, 2023; accepted January 29, 2024

Lactate–proton symporter monocarboxylate transporter 1 (MCT1) facilitates lactic acid export from T cells. Here, we report that MCT1 is mandatory for the development of virus-specific CD8$^+$ T cell memory. MCT1-deficient T cells were exposed to acute pneumovirus (pneumonia virus of mice, PVM) or persistent γ-herpesvirus (Murid herpesvirus 4, MuHV-4) infection. MCT1 was required for the expansion of virus-specific CD8$^+$ T cells and the control of virus replication in the acute phase of infection. This situation prevented the subsequent development of virus-specific T cell memory, a necessary step in containing virus reactivation during γ-herpesvirus latency. Instead, persistent active infection drove virus-specific CD8$^+$ T cells toward functional exhaustion, a phenotype typically seen in chronic viral infections. Mechanistically, MCT1 deficiency sequentially impaired lactic acid efflux from activated CD8$^+$ T cells, caused an intracellular acidification inhibiting glycolysis, disrupted nucleotide synthesis in the upstream pentose phosphate pathway, and halted cell proliferation which, ultimately, promoted functional CD8$^+$ T cell exhaustion instead of memory development. Taken together, our data demonstrate that MCT1 expression is mandatory for inducing T cell memory and controlling viral infection by CD8$^+$ T cells.

T cell memory development | T cell exhaustion | lactate transport | monocarboxylate transporters (MCTs) | virus latency

Significance

Rapidly proliferating cells switch from oxidative phosphorylation to aerobic glycolysis, dramatically increasing glucose catabolism. The MCT1 transporter is involved in the extrusion of lactic acid, the end product of glycolysis, from T cells after activation. Our study shows that limited expansion of virus-specific MCT1-deficient CD8$^+$ T cells prevents the development of T cell memory, normally required for the control of γ-herpesvirus reactivation during latency. Instead, uncontrolled viral replication induced functional exhaustion of MCT1-deficient CD8$^+$ T cells, a condition commonly associated with chronic infections. Thus, lactate export is essential for the development of protective memory T cells required to prevent viral latency from turning into chronic infection.

By eliminating infected cells, T cells are key players in controlling viral infection. However, when host immune responses fail to control virus replication, persistent exposure to viral antigens induces functional exhaustion in T cells, characterized by failing effector functions and reduced proliferative potential (1). Exhausted T cells (Tex) are distinct in terms of molecular signatures, including overexpression of inhibitory receptors, altered cytokine signaling, and dysregulated metabolism (2–4). The reactivation of Tex can be induced by blocking cell surface inhibitory receptors (1). Recent studies indicate, however, that Tex ability to respond to treatment depends largely on their stage of development which is tightly controlled by the combined activity of transcription factors (2, 5). This is how self-replicating TCF1$^+$ Tex progenitors give rise to an intermediate TCF1$^-$ Tbet^{hi} Tex subpopulation capable of reacquiring some effector-like functions after inhibitory receptor blockade (2, 5). These cells, however, ultimately develop into short-lived terminally exhausted Tbet$^-$ TOX$^+$ Tex, poorly responding to therapies aimed at restoring T cell function (2, 5).

Immune exhaustion is not the only mechanism that allows viruses to evade T cells. Herpesviruses and in particular γ-herpesviruses have coevolved with their host for many years in such a way as to establish a prevalent persistent infection in humans. This persistence throughout life is linked to different mechanisms, including escape from neutralizing specific antibodies, the development of immunomodulatory responses, and the establishment of latency (6–8). Latency is intimately associated with the development of an effective and long-lasting cytotoxic response mediated by T lymphocytes (9). The phenotype of antigen-specific T cells in γ-herpesvirus infections is effector-memory-like, characterized by low expression levels of CD62L and CD127. In contrast to Tex, KLRG1 is highly expressed, whereas the expression of inhibitory receptors, such as PD-1, is low (10–12). Potential causes of persistent viral infection to elicit either T cell–controlled viral latency or long-lasting viral replication that maintains T cell exhaustion are unclear. Nevertheless, available evidence indicates that strong viral replication in the onset of infection promotes virus persistence and drives T cell exhaustion (13), while early vigorous expansion of virus-specific T cells is needed to promote virus latency (14–16). Moreover, sustained antigen expression maintains T cell exhaustion (17, 18), whereas intermittent viral replication with limited periods of antigen presence retains functional T cells with the capacity to impose virus latency (19).

Author contributions: F.A., P.S., B.M., L.G., and M.Y.B. designed research; S. D'Aria, C.M., S.L., A.L., A.K., M.F., and I.N. performed research; S. Dhup, V.F.V.H., and R.K.D. contributed new reagents/analytic tools; S. D'Aria, C.M., S.L., F.A., I.N., P.S., B.M., L.G., and M.Y.B. analyzed data; and P.S., B.M., L.G., and M.Y.B. wrote the paper.

The authors declare no competing interest.

This article is a PNAS Direct Submission.

[1]S. D'Aria, C.M., and S.L. contributed equally to this work.

[2]P.S., B.M., L.G., and M.Y.B. contributed equally to this work.

[3]To whom correspondence may be addressed. Email: michel.braun@ulb.be.

This article contains supporting information online at https://www.pnas.org/lookup/suppl/doi:10.1073/pnas.2306763121/-/DCSupplemental.

Published March 18, 2024.

Upon activation, T cells shift toward a metabolism characterized by increased glucose metabolism in order to sustain proliferation and effector functions (20). Since activated T lymphocytes engage in glycolysis, they must release lactate, which is facilitated by proton-linked monocarboxylate transporters (MCTs) (21). MCTs are, however, passive transporters, antagonized by the high levels of lactic acid found in glycolytic tissues (21). The high affinity for lactate displayed by MCT1 makes it a very valuable transporter in situations where the lactate gradient across the plasma membrane is low. On the one hand, the observation that pharmacological inhibition (22) of MCT1 limits proliferation in T cells suggests that lactate extrusion through MCT1 is essential for T cell expansion triggered by antigen recognition. On the other hand, MCT1-mediated lactate uptake was shown to be required for the function of T regulatory cells present in the tumor microenvironment (23, 24). Moreover, lactate oxidation was recently shown to reduce glucose contribution to the TCA in $CD8^+$ T cells responding to Listeria infection (25). Thus, under particular circumstances, extracellular lactate may represent a source of fuel in T cells where it is converted by LDH to pyruvate (25).

In the present study, T cell–specific deletion of the MCT1/Slc16a1 gene was used to investigate how modulating lactate transport in virus-specific T cells could affect infection. We show that MCT1 deficiency in T cells prevented the development of a protective immunity against acute viral infection, identifying lactate transport by MCT1 as a critical factor for T cell–mediated antiviral responses. More surprising was the observation, in a mouse model of γ-herpesvirus latent infection, that the absence of MCT1 in T cells was associated with increased frequencies of viral reactivation episodes and the emergence of functional exhaustion among virus-specific $CD8^+$ T cells.

Results

MCT1 Expression Is Required for Optimal Proliferation of $CD8^+$ T Cells. In order to address the role of MCT1/Slc16a1 gene in T cells upon in vitro and in vivo activation, we used B6.Slc16a1$^{fl/fl}$.CD4^{Cre} mice. With regard to their subpopulations of thymocytes and resting peripheral $CD4^+$ and $CD8^+$ T lymphocytes, B6.Slc16a1$^{fl/fl}$.CD4^{Cre} mice (KO mice) were not different from B6.Slc16a1$^{fl/fl}$ mice (WT) or B6 mice (*SI Appendix*, Fig. S1). As previously reported (26), MCT1 expression was up-regulated early after stimulation in WT T cells (Fig. 1*A*). However, failure to express MCT1 in KO T cells (Fig. 1*B* and *SI Appendix*, Fig. S2*A*) was not compensated by increased expression of MCT4 (Fig. 1*C* and *SI Appendix*, Fig. S2*B*), the other MCT isoforms expressed by mouse T cells (26). As expected, activated KO $CD8^+$ T cells showed limited proliferation (Fig. 1*D*). In contrast, their capacity to produce IFNγ after activation was unaffected by the loss of MCT1 (Fig. 1*E* and *SI Appendix*, Fig. S3). Likewise, their expression of other effector genes such as those for perforin and granzyme B was not modified (*SI Appendix*, Fig. S4 *A* and *B*). Unlike $CD8^+$ T cells, the proliferative capacity of $CD4^+$ T lymphocytes was only marginally modified by the loss of MCT1 expression (*SI Appendix*, Fig. S2*C*), confirming previous observations that only $CD8^+$ T cell proliferation depends on MCT1 expression (22, 27). The capacity of $CD4^+$ T cells to

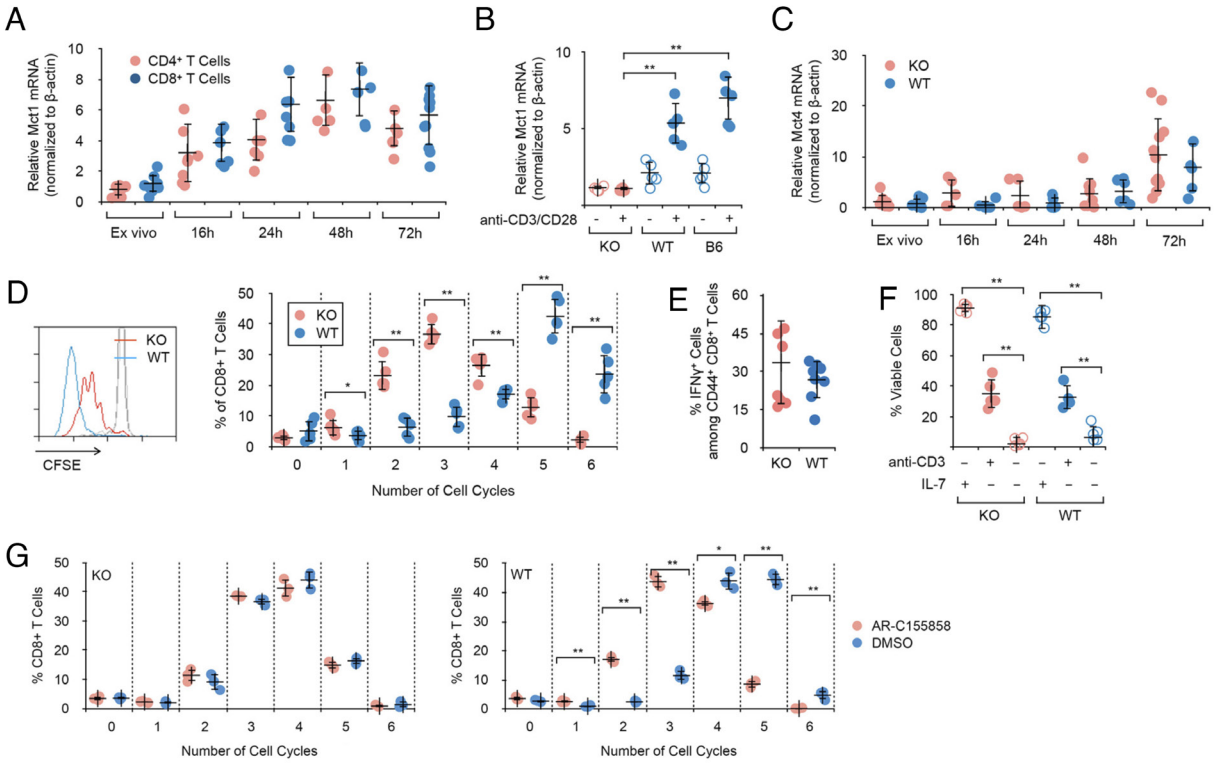

Fig. 1. MCT1 expression is required for optimal proliferation of activated $CD8^+$ T cells. (*A*) *Mct1* mRNA expression in spleen $CD4^+$ and $CD8^+$ T cells isolated from B6 mice and stimulated with anti-CD3/CD28 antibodies for the indicated time points. n = 5 to 8 mice per group. (*B*) *Mct1* mRNA expression in spleen $CD8^+$ T cells isolated from KO, WT, and B6 mice and stimulated with anti-CD3/CD28 antibodies for 72 h. n = 5 mice per group. $^{**}P < 0.01$. (*C*) *Mct4* mRNA expression in spleen $CD8^+$ T cells isolated from KO and WT mice and stimulated with anti-CD3/CD28 antibodies for the indicated time points. n = 4 to 12 mice per group. (*D*) Flow cytometry analysis of CFSE-stained KO and WT spleen cells after 72-h in vitro stimulation with soluble anti-CD3 antibodies. Percent within viable $CD8^+$ TcRα,β^+ cells from individual mice is shown for each cell cycle. n = 5 mice per group. $^{**}P < 0.01$; $^{*}P < 0.05$. (*E*) Flow cytometry analysis of purified KO and WT $CD8^+$ T cells for their capacity to produce IFNγ after stimulation for 72 h with anti-CD3/CD28 antibodies. n = 7 to 8 mice per group. (*F*) Percent of viable KO and WT $CD8^+$ TcRα,β^+ spleen cells after 72 h of culture alone, with IL-7 or stimulated as in (*A*). n = 5 mice per group. $^{**}P < 0.01$. (*G*) Flow cytometry analysis of CFSE-stained spleen cells stimulated by anti-CD3 antibodies for 72 h in the presence of MCT1 inhibitor AR-C155858 or carrier (DMSO) alone. Percent within viable $CD8^+$ TcRα,β^+ cells from individual mice is shown for each cell cycle. n = 3 mice per group. $^{**}P < 0.01$; $^{*}P < 0.05$.

differentiate into Th subsets was also unaffected by the lack of MCT1 expression (*SI Appendix*, Fig. S5). As indicated in Fig. 1*F*, reduced proliferation of KO CD8$^+$ T cells was not the result of poorer cell viability. Moreover, adding IL-7, a major cytokine for the survival of resting T cells, equally protected unstimulated WT and KO T cells against cell death (Fig. 1*F*). Whereas AR-C155858, a specific MCT1 inhibitor (22), significantly inhibited the proliferation of activated WT CD8$^+$ T cells, it did not impact that of KO CD8$^+$ T cells, demonstrating that inhibition of proliferation was a direct consequence of MCT1 deficiency (Fig. 1*G*). Taken together, these results demonstrate that MCT1 expression is required for optimal proliferation of activated CD8$^+$ T cells, whereas it appears to be optional for activated CD4$^+$ T cells.

MCT1 Expression Potentiates CD8$^+$ T Cells for the Control of Viral Acute Infection. The immune outcome of viral infection largely depends on the ability of T cells to proliferate (28). To interrogate the importance of MCT1 expression in antiviral T cell responses, we first analyzed MCT1-deficient CD8$^+$ T cells for their capacity to respond to acute infection by pneumonia virus of mice (PVM) (Fig. 2*A*). Unlike γ-herpesviruses, PVM causes a silent infection in immunocompetent mice, and CD8$^+$ T cells play a prominent role in eradicating PVM infections (29–31). MCT1 deficiency in T cells resulted in a sharp increase in sensitivity to PVM infection as evidenced by increased weight loss and poorer survival in KO mice (Fig. 2 *B* and *C*). Strikingly, after 8 d, very few PVM-specific CD8$^+$ T cells were detected in the lung, mediastinal lymph nodes (MLN), or spleen of infected KO mice, contrasting with the strong expansion of PVM-specific WT CD8$^+$ T cells (Fig. 2*D* and *SI Appendix*, Fig. S6). Conversely, the viral load in the lungs of KO mice was two to three times higher than that of WT mice (Fig. 2*E*). Taken together, these results demonstrated that, due to their limited proliferation after activation, CD8$^+$ T cells lacking MCT1 expression were unable to participate in the control of acute PVM infection. As a result, the relative numbers of CD8$^+$ T cells in the lungs of infected mice that expressed effector proteins such as IFNγ and granzyme B were also low (Fig. 2*F*).

As mentioned in the introduction, early control of viral replication is a prerequisite for promoting viral latency, and virus-specific CD8$^+$ T cells play an important role in controlling the acute phase of infection by murid herpesvirus 4 (MuHV-4) in the mouse (32). Since lack of MCT1 expression inhibited CD8$^+$ T cells for controlling early PVM infection, how this might affect the primary response toward MuHV-4 was investigated. Unlike in the PVM infection model, reduced survival was not seen in KO mice infected with MuHV-4, although slight weight loss was noticed (Fig. 2 *G–I*). At day 8 postinfection, however, the numbers of MuHV-4-specific MCT1-deficient CD8$^+$ T cells present in infected mice were very low (Fig. 2*J* and *SI Appendix*, Fig. S6). This situation was inversely correlated with the higher viral load present in the lungs of KO mice (Fig. 2*K*). Thus, similar to what was observed with acute PMV infection, low number of MuHV-4-specific MCT1-deficient CD8$^+$ T cells was correlated with high viral replication. Specific differences, however, were observed. Unlike their PVM-specific counterparts, MuHV-4-specific MCT1-deficient CD8$^+$ T cells retained most of their effector function, with a normal expression of granzyme B and a slight decrease in the production of IFNγ (Fig. 2*L*). Taken together, these results demonstrated that MCT1 expression by virus-specific CD8$^+$ T cells is required for controlling the acute phase in MuHV-4 infection.

Because the use of CD4-Cre deletes MCT1 expression in CD8$^+$ T cells as well as in CD4$^+$ T cells, it was possible that the limited expansion of virus-specific MCT1-deficient CD8$^+$ T cells was not cell intrinsic but originated from a skewed expansion or differentiation of CD4$^+$ T cells that would limit their auxiliary activity toward CD8$^+$ T cells. To address this question, we generated bone marrow (BM) chimera in irradiated hosts by cotransferring an equal mix of BM cells from T cell conditional *Slc16a1* KO and congenic WT controls (Fig. 3 *A* and *B*). After MuHV-4 infection, lung T cells were assessed for their ability to proliferate, their activation status, and specific antiviral response. As depicted in Fig. 3*C*, the number of both CD8$^+$ and CD4$^+$ T cells present in the lung increased after infection. However, whereas the proportion of lung WT vs. KO T cells was similar in uninfected controls, it was significantly increased in MuHV-4-infected recipients (Fig. 3*D*). Analysis of T cell expansion by the mean of Ki67 expression indicated that pulmonary MCT1-deficient CD8$^+$ T cells proliferated less than WT CD8$^+$ T cells (Fig. 3*E*). This difference was, however, not seen among CD4$^+$ T cells (Fig. 3*E*). Moreover, after infection, activated MCT1-deficient CD8$^+$ T cells, as defined by their expression of the surface activation markers CD44, Ly6C, and CD69, were less present than WT cells in the lung of infected mice (Fig. 3 *F–H*). In contrast, while KO CD4$^+$ T cells displayed a slight reduction of proliferation (Fig. 3*E*), we did not observe any difference in the proportion of activated cells between WT and KO engrafted CD4$^+$ T cells (Fig. 3 *F–H*). These observations supported the fact that lack of MCT1 expression primarily affects CD8+ T cell proliferation in a cell-intrinsic manner. Accordingly, MuHV-4-specific as well as IFNγ-producing MCT1-deficient CD8$^+$ T cells were less present in the lung of infected recipients (Fig. 3 *I–K*). Interestingly, activation and proliferation of NKT cells, which also lack MCT1 in these CD4-Cre mice, were not affected by the loss of MCT1 expression (*SI Appendix*, Fig. S7).

MCT1 Expression in T Cells Is Required for Induction and Long-Term Maintenance of Viral Latency. Expansion of virus-specific T cells early upon infection is required to promote MuHV-4 latency (32). In infected mice, MuHV-4 replication peaks in the lungs on day 7 postinfection and becomes undetectable by the time viral latency is established (33). As shown in Fig. 4 *B* and *C*, viral replication, as assessed by luciferase activity (34), was robust in the lungs of KO mice at day 7, confirming that MCT1-deficient T cells did not control acute infection. However, analysis of luciferase activity 4 mo later revealed sustained viral replication in several organs of KO mice while, as expected, it was absent in WT animals (Fig. 4 *B* and *C*). The expression of viral luciferase in KO mice was correlated with the detection of a high number of MuHV-4 genome copies in the lungs and spleens of KO mice (Fig. 4*D*). Taken together, these observations demonstrated that MCT1 expression by CD8$^+$ T cells is necessary for controlling viral replication and the fine regulation between lytic cycle and latency.

MCT1 Expression in CD8$^+$ T Cells Prevents Viral Latency from Turning into Chronic Infection. Contrary to what is seen during viral latency, sustained antigenic stimulation drives functional exhaustion in CD8$^+$ T cells during chronic viral infection (17). Since MuHV-4 replication was strong all along the experiment in KO mice (Fig. 4 *B* and *C*), we examined virus-specific MCT1-deficient CD8$^+$ T lymphocytes for possible phenotypic modifications associated with exhaustion. At day 30, MCT1-deficient CD8$^+$ T cells isolated from the lungs and spleen of infected mice exhibited a low capacity to produce IFNγ, consistent with an exhaustion phenotype (*SI Appendix*, Fig. S8 *A* and *B*). This was correlated with a higher number of viral genome copies in the lungs (*SI Appendix*, Fig. S8*C*). However, contrary to what was observed in the acute phase, the relative number of virus-specific CD8$^+$ KO T cells was twice as high as that of WT CD8+ T cells in the lungs and spleen of infected mice (*SI Appendix*, Fig. S8*D*).

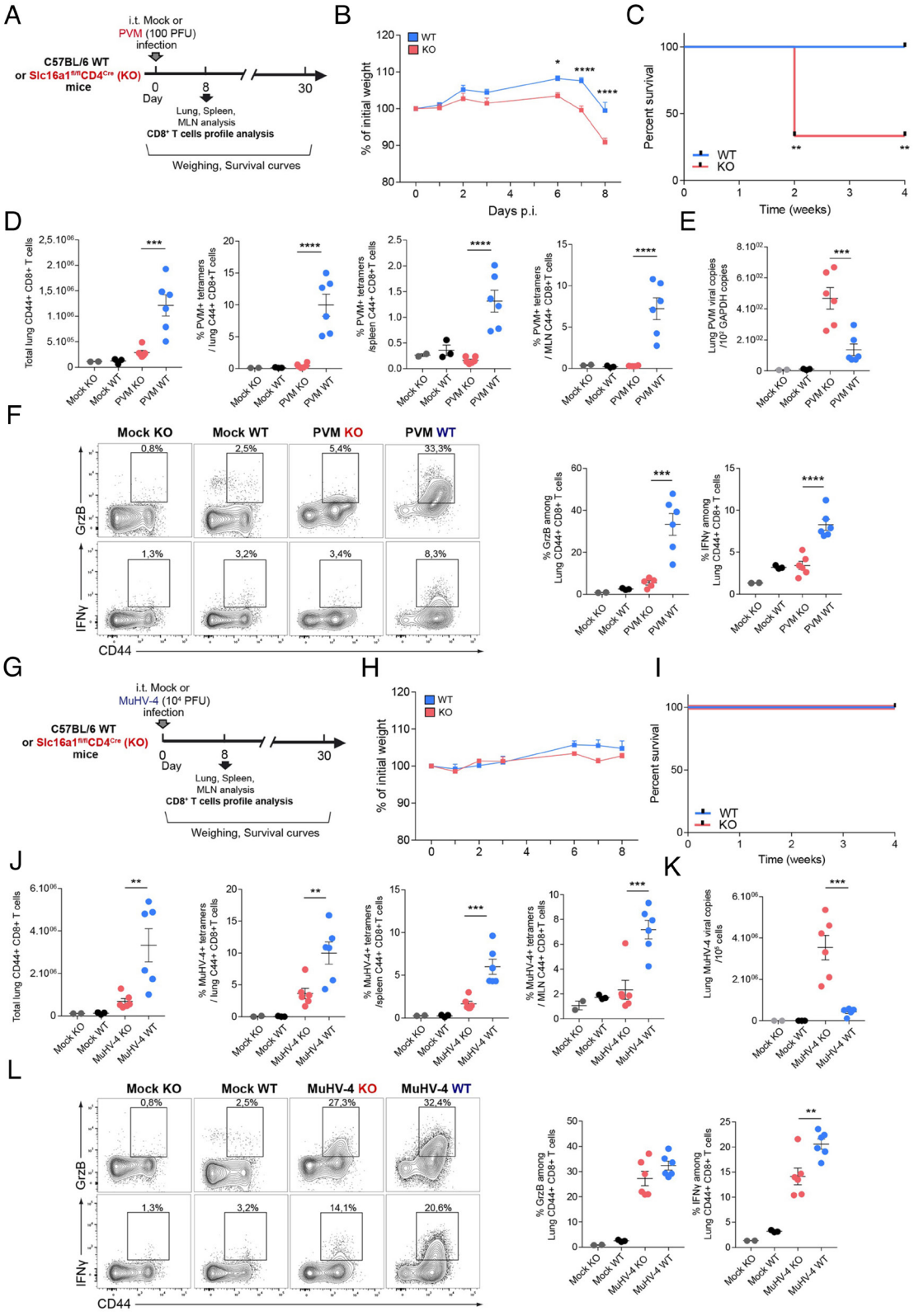

Fig. 2. MCT1 expression is required for CD8$^+$ T cells to control acute viral infection. (*A*) Protocol of PVM infection and experimental timeline. (*B*) Percent of initial body weight of MCT1-deficient (KO) and WT mice after intratracheal infection with PVM. n = 6 mice per group. ***$P < 0.0001$; *$P < 0.05$. (*C*) Percent of survival of KO and WT mice after intratracheal infection with PVM. n = 6 mice per group. **$P < 0.01$. (*D*) Relative numbers of virus-specific cells among CD44$^+$ CD62L$^-$ CD8$^+$ T cells in the lung, spleen, and MLN of PVM-infected KO and WT mice. n = 6 mice per group. ****$P < 0.0001$; ***$P < 0.001$. (*E*) Virus copy numbers detected in the lung of PVM-infected KO and WT mice. n = 6 mice per group. ***$P < 0.001$. (*F*) Relative numbers of granzyme B$^+$ and IFNγ$^+$ cells among CD44$^+$ CD62L$^-$ CD8$^+$ T cells in the lung of PVM-infected KO and WT mice. n = 6 mice per group. ****$P < 0.0001$; ***$P < 0.001$. (*G*) Protocol of MuHV-4 infection and experimental timeline. (*H*) Percent of initial body weight of MCT1-deficient (KO) and WT mice after intratracheal infection with MuHV-4. n = 6 mice per group. (*I*) Percent of survival of KO and WT mice after intratracheal infection with MuHV-4. n = 6 mice per group. (*J*) Relative numbers of virus-specific cells among CD44$^+$ CD62L$^-$ CD8$^+$ T cells in the lung, spleen, and MLN of MuHV-4-infected KO and WT mice. n = 6 mice per group. ***$P < 0.001$; **$P < 0.01$. (*K*) Virus copy numbers detected in the lung of MuHV-4-infected KO and WT mice. n = 6 mice per group. ***$P < 0.001$. (*L*) Relative numbers of granzyme B$^+$ and IFNγ$^+$ cells among CD44$^+$ CD62L$^-$ CD8$^+$ T cells in the lung of MuHV-4-infected KO and WT mice. n = 6 mice per group. **$P < 0.01$.

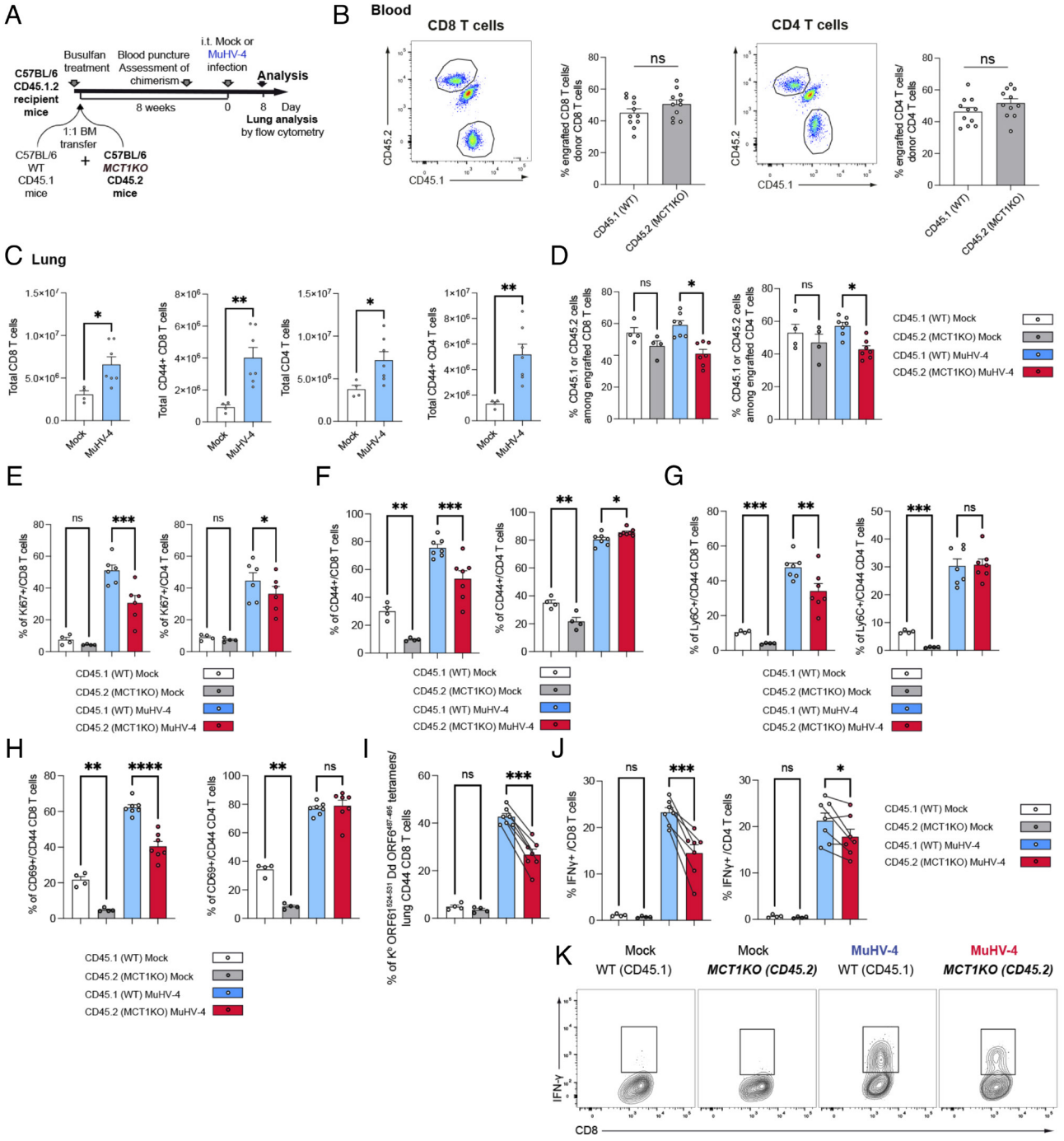

Fig. 3. The limited expansion of virus-specific MCT1-deficient CD8$^+$ T cells is cell intrinsic. (*A*) Experimental layout. (*B*) Control of engraftment of donor CD8$^+$ and CD4$^+$ T cells respective from WT (CD45.1) and MCT1 KO (CD45.2) compartments in the blood 6 wk post-reconstitution. (*C*) Total lung CD8$^+$ and CD4$^+$ T cells at day 8 post-MuHV-4 infection. (*D*) Control of engraftment of donors CD8$^+$ and CD4$^+$ T cells respective from WT (CD45.1) and MCT1 KO (CD45.2) compartments in the lungs 8 d postinfection. (*E–H*) Percentages of donor lung CD8$^+$ and CD4$^+$ T cells expressing Ki67 (*E*), CD44 (*F*), Ly6C (*G*), and CD69 (*H*) activation markers at day 8 p.i. (*I*) Percentages of donor CD8$^+$ T cells recognizing DbORF6$^{487-495}$ and KbORF61$^{524-531}$ MuHV-4-specific epitopes among CD44$^+$ CD62L$^-$ CD8$^+$ T cells in the lung. Lines linked paired measurements in the CD45.1 and CD45.2 compartments within individual mice. (*J* and *K*) Percentages (*J*) and FACS plots (*K*) of donor IFNγ-expressing lung CD8 T cells. Lines linked the differences between the CD45.1 and CD45.2 compartments within individuals. Data were analyzed by the two-tailed paired *t* test (ns: not significant, **P* < 0.05, ***P* < 0.01, ****P* < 0.001, and *****P* < 0.0001). Error bars represent SEM.

Unlike most WT CD8$^+$ T cells, about 10 to 20% of KO CD8$^+$ T cells isolated from the lung and spleen of infected mice expressed PD1 (*SI Appendix*, Fig. S8 *E–G*). Moreover, most of the cells were PD1^{high} CD69^{high} (*SI Appendix*, Fig. S8 *E–G*), a phenotype that characterizes terminally exhausted Tex (2). Taken together these observations suggested that continuous higher viral replication was responsible for the persistence of MCT1-deficient CD8$^+$ Tex. At 120 d after infection, MuHV-4-specific CD8$^+$ T cells were three to four times more abundant in the lungs and spleen of KO mice than in those of WT counterparts (Fig. 4*E*). In addition, beside PD1 (Fig. 4 *F* and *G*), other exhaustion markers, such as CD101 (5), TIM-3 (35) and nuclear factor TOX (36–38) were found expressed by MCT1-deficient CD8$^+$ T cells isolated from infected KO mice (Fig. 4 *H* and *I*), demonstrating that these cells were indeed functionally exhausted. Moreover, as observed after 30 d, many of the CD8$^+$ T cells, mostly from the lung, were PD-1^{high}

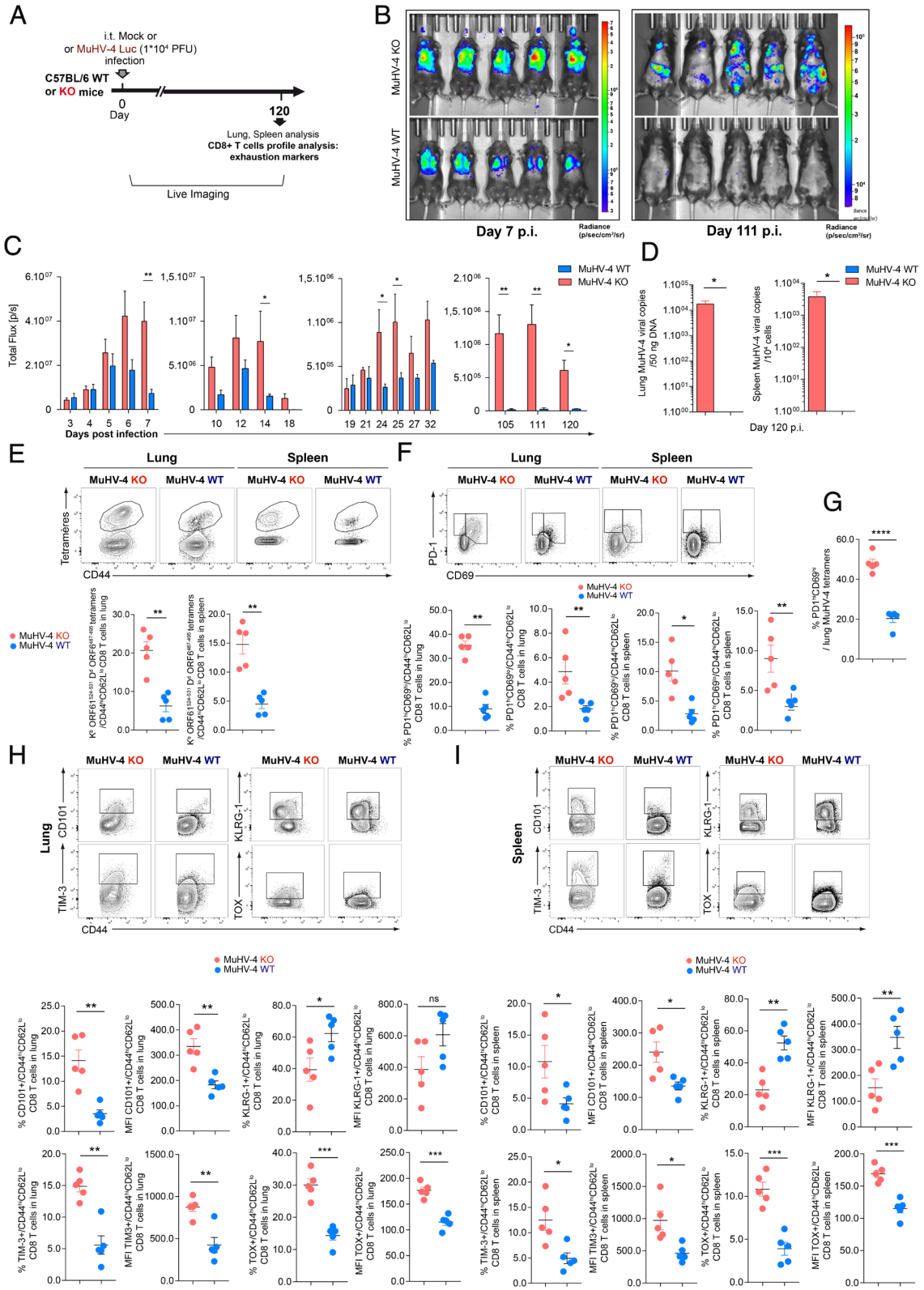

Fig. 4. MCT1 expression by CD8$^+$ T cells is required to promote viral latency. (*A*) Protocol of MuHV-4 infection and experimental timeline used to study viral latency. (*B*) In vivo imaging of viral replication by luciferase-transgenic MuHV-4 after injection of D-luciferin and capture of photon emission at 7 and 111 d postinfection. (*C*) Time course of viral replication visualized by in vivo imaging as in (*B*). n = 5 mice per group. $^{**}P < 0.01$; $^{*}P < 0.05$. (*D*) Virus copy numbers detected in the lung of MuHV-4-infected KO and WT mice 120 d after infection. n = 5 mice per group. $^{*}P < 0.01$. (*E*) Relative numbers of virus-specific cells among CD44$^+$ CD62L$^-$ CD8$^+$ T cells in the lung and spleen of MuHV-4-infected KO and WT mice 120 d after infection. n = 5 mice per group. $^{**}P < 0.01$. (*F*) Expression of PD-1 and CD69 by CD44$^+$ CD62L$^-$ CD8$^+$ T cells in the lung and spleen of MuHV-4-infected KO and WT mice. n = 5 mice per group. $^{**}P < 0.01$; $^{*}P < 0.05$. (*G*) Expression of PD-1 and CD69 by tetramer-positive CD8$^+$ T cells in the lung of MuHV-4-infected KO and WT mice. n = 5 mice per group. $^{****}P < 0.0001$. (*H*) Expression of CD101, TIM-3, KLRG1, and TOX by CD44$^+$ CD62L$^-$ CD8$^+$ T cells in the lung of MuHV-4-infected KO and WT mice. n = 5 mice per group. $^{***}P < 0.001$; $^{**}P < 0.01$; $^{*}P < 0.05$. (*I*) Expression of CD101, TIM-3, KLRG1, and TOX by CD44$^+$ CD62L$^-$ CD8$^+$ T cells in the spleen of MuHV-4-infected KO and WT mice. n = 5 mice per group. $^{***}P < 0.001$; $^{**}P < 0.01$; $^{*}P < 0.05$.

and coexpressed CD69, a phenotype consistent with terminal exhaustion (2) (Fig. 4 *F* and *G*). On the contrary, $CD8^+$ T cells isolated from the lungs and spleen of infected WT mice were predominantly $KLRG1^{high}$, a feature of late-differentiated effector memory $CD8^+$ T cells (11, 39) (Fig. 4 *H* and *I*). Thus, MCT1 expression by virus-specific $CD8^+$ T cells is required for silencing viral replication that characterizes MuHV-4 latency.

Altered Glycolytic Metabolism in Activated MCT1-Deficient T Cells. The cause of the limited proliferation observed in activated MCT1-deficient $CD8^+$ T cells was investigated. Consistent with glycolysis being a major metabolic pathway for proliferation, lactate, the end product of glycolysis, was less present in cultures of activated MCT1-deficient $CD8^+$ T cells (Fig. 5*A*). Accordingly, since MCT-mediated lactate transport across cell membranes is carried out by diffusional cotransport with protons, the culture medium of activated KO T cells was less acidic than that of WT counterparts (Fig. 5*B*). The observation that activated $CD8^+$ KO T cells were more stained by the cytoplasmic pH indicator pHrodo also supported the idea that lack of MCT1 expression limited lactate export (Fig. 5*C*). Glycolytic activities of KO and WT $CD8^+$ T cells were assessed by their extracellular acidification rate (ECAR). Unstimulated $CD8^+$ T cells showed negligible ECAR (Fig. 5*D*), regardless of the MCT1 expression status. However, after 48 h activation, KO T cells displayed systematically lower basal ECAR of their WT counterparts (Fig. 5*D*). The maximum glycolytic capacity displayed by WT T cells after the addition of oligomycin doubled that of KO T cells (Fig. 5*D*), demonstrating that KO T cells were less glycolytic than WT T cells. After 72 h, maximum ECARs displayed by KO and WT T cells were almost identical, suggesting that the late increased expression of MCT4 that we observed after activation restored partially their glycolytic capacity (Fig. 5*D*). However, basal ECAR of KO T cells at that time point was still below that of WT T cells (Fig. 5*D*). The lycolytic activity of T cells can also be assessed by analyzing mRNA translation levels by puromycin incorporation upon blockade of different metabolic pathways (Fig. 5 *E* and *F* and *SI Appendix*, Fig. S9) (40). Using immunofluorescence to detect puromycin incorporation levels, the basal metabolism of the cells can be measured at the single-cell level by flow cytometry (*SI Appendix*, Fig. S9). As shown in Fig. 5*G*, unstimulated or anti-CD3-stimulated KO and WT $CD8^+$ T cells could not be differentiated based on the levels of their basal metabolism. After the addition of oligomycin, which blocks oxidative phosphorylation (OXPHOS) and causes T cells to use only glycolysis for protein synthesis, the glycolytic capacity of KO and WT $CD8^+$ T cells can be calculated as a percentage of the basal cellular metabolism (Fig. 5*F*). Unstimulated, both types of cells exhibited low levels of glycolytic capacity (Fig. 5*H*). After stimulation, these increased rapidly (Fig. 5*H*). The increase was, however, much greater in WT T cells, reaching a level twice that of KO T cells after 48 h of stimulation (Fig. 5*H*). Blocking the entry of glucose using 2-DG allowed the evaluation of the dependence of T cells on both glucose and on amino acids and fatty acids (Fig. 5 *I* and *J*). As depicted in Fig. 5*I*, both types of cells relied mostly on glucose for their metabolism. However, glucose dependence was more marked in WT T cells than in KO T cells after stimulation (Fig. 5*I*). On the contrary, the dependence on amino acids and/or fatty acids as an energy source for biosynthesis increased after stimulation in KO T cells whereas it decreased in WT cells (Fig. 5*J*). Taken together, these results supported the notion that, after stimulation, KO $CD8^+$ T cells were delayed relative to WT $CD8^+$ T cells in their initiation of glycolysis. On the contrary, activated KO T cells appeared to rely more on amino acid (AAO) and fatty acid (FAO) oxidation, suggesting that OXPHOS might be used to compensate a deficient glycolysis.

Metabolomic analysis by LC/MS-MS revealed, however, that, despite lower glycolysis, activated MCT1-deficient $CD8^+$ T cells accumulated glycolytic intermediates, including glucose 6-phosphate, dihydroxyacetone phosphate, glyceraldehyde 3-phosphate, pyruvate and lactate, as well as sedoheptulose 7-phosphate from the pentose phosphate pathway (Fig. 6 *A*–*C*). Phosphoenolpyruvate (PEP) was also builded up in MCT1-deficient T cells (2.85-fold), although this difference did not reach significance. It is known that glycolytic intermediates accumulate intracellularly in cancer cells following pharmacological inhibition of lactate export (41, 42). However, this situation is usually accompanied by a marked reduction of products of the ATP-generating arm of glycolysis, including PEP and pyruvate (41, 42). This was clearly not the case for KO T cells since both intermediates accumulated in stimulated MCT1-deficient $CD8^+$ T cells (Fig. 6 *B* and *C* and *SI Appendix*, Table S1). Pathway analysis confirmed that the pentose phosphate pathway and glycolysis were the most significantly disrupted by the absence of MCT1 (Fig. 6*D*). Targeted LC-MS analysis also indicated that KO and WT T cells could not be differentiated based on the amount of glucose they contained (Fig. 6*E*). This was confirmed by analyzing the incorporation of the fluorescent glucose derivative 2-Deoxy-D-glucose (2-DG) (*SI Appendix*, Fig. S4*G*). Moreover, the upregulation of glucose transporter GLUT1 mRNA expression after activation was equivalent in activated WT and KO T cells, making it unlikely that lower glucose uptake would be responsible for the reduced proliferation of activated KO T cells (*SI Appendix*, Fig. S4*C*). Expression of glycolytic enzymes, known to increase in T cells following activation (43), was also not different between activated KO and WT $CD8^+$ T cells (*SI Appendix*, Fig. S4 *D*–*F*). Taken together, these results supported the notion that the decreased glycolytic activity observed in activated $CD8^+$ KO T cells was not caused by a lower expression of glycolytic enzymes or glucose transporters but rather by a negative feedback loop mediated by accumulating glucose-derived metabolites.

MCT1 Expression Is Required for Nucleotide Synthesis in Activated $CD8^+$ T Cells. Compared to the situation in WT T cells, a significant accumulation of cis-aconitate as well as maintained levels of citrate and α-ketoglutarate (αKG) were observed in MCT1-deficient T cells after activation (Fig. 6 *E* and *F*). This contrasted with four-carbon intermediates, succinate, fumarate, and malate, which were strongly depleted (Fig. 6 *E* and *F*). This implies that glucose-derived pyruvate was oxidized, but that oxidation stopped at the step leading to αKG. Interestingly, though glutamine levels were unchanged, glutamate was strongly depleted in activated MCT1-deficient $CD8^+$ T cells (Fig. 6 *E* and *F*). These observations supported the idea that the decarboxylation of glutamate to succinate by the GABA (gamma-amino-butyrate) shunt of the glutamine pathway could be specifically implemented in KO $CD8^+$ T cells to maintain cellular energy production when αKG dehydrogenase complex (KGDH) was inhibited (44). KGDH is particularly sensitive to inhibition when the energy load, or [ATP]/[ADP] ratio, is high (45, 46). Interestingly, cellular energy load was higher in activated MCT1-deficient $CD8^+$ T cells (Fig. 6*G*). This did not result from increased ATP production. Both KO and WT $CD8^+$ T cells saw their ATP levels dropping sharply after 12 h of stimulation, highlighting an intense use of ATP during the initial steps of cellular proliferation (Fig. 6*H*). This was followed by a stage where ATP synthesis would exceed its use, allowing the reconstitution of cellular energy reserve (Fig. 6*H*). Both KO and WT T cells exhibited similar kinetics of ATP reconstitution (Fig. 6*H*). Accordingly, LC-MS analysis confirmed that MCT1 deficiency did not deplete the overall ATP levels in $CD8^+$ T cells after stimulation (Fig. 6 *F* and *I*). Taken together, these results

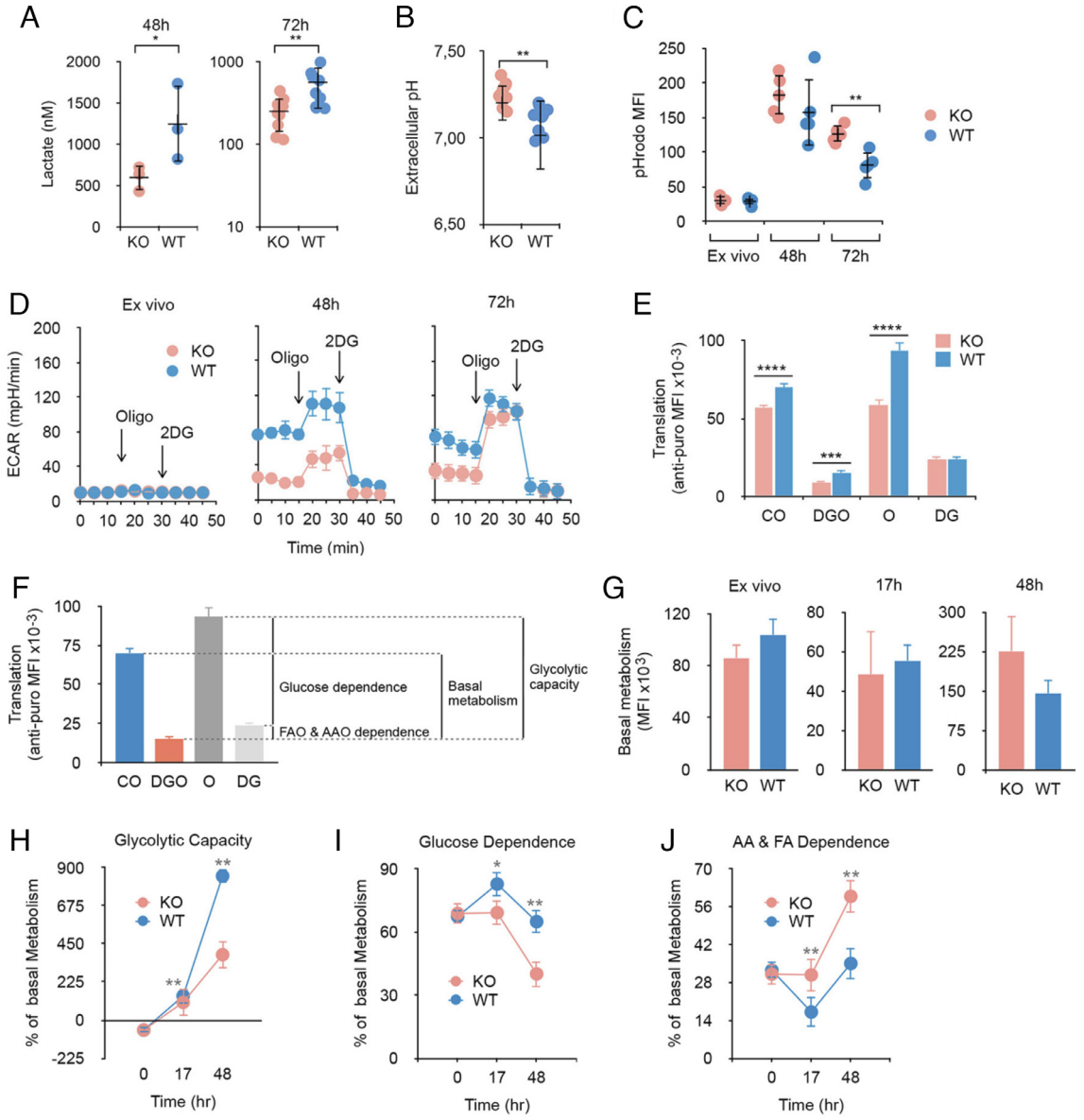

Fig. 5. Low level of glycolysis in activated MCT1-deficient CD8$^+$ T cells. (*A*) Dosage of lactate present in culture supernatants of spleen CD8$^+$ T cells from KO and WT mice and stimulated with anti-CD3/CD28 antibodies for 48 h or 72 h. n = 3 to 9 mice per group. $^{**}P < 0.01$; $^{*}P < 0.05$. (*B*) Extracellular pH of culture medium after 72 h anti-CD3/CD28-mediated stimulation of CD8$^+$ T cells from KO and WT mice. n = 8 mice per group. $^{**}P < 0.01$. (*C*) Cytoplasmic acidity was assessed by staining KO and WT CD8$^+$ T cells with pHRodo before and after stimulation with anti-CD3/CD28 antibodies and rIL-2 for 48 h and 72 h. n = 5 mice per group $^{**}P < 0.01$. (*D*) Extracellular acidification rate (ECAR) of CD8$^+$ T cells purified from the spleen of KO and WT mice and stimulated with anti-CD3/CD28 antibodies for 48 h or 72 h. Data shown are representative of three independent experiments. (*E*) Translation (puromycin incorporation) assessment in KO and WT CD8$^+$ T cells stimulated as in (*E*). Puromycin incorporation was assessed by measuring the MFI of staining carried out with Alexa Fluor-conjugated anti-puromycin antibodies. CO: control incorporation without inhibitors; DG: incorporation after inhibition by 2-DG; O: incorporation after inhibition with oligomycin; DGO: incorporation after inhibition with both 2-DG and oligomycin. n = 4 mice per group. $^{****}P < 0.0001$; $^{***}P < 0.001$. (*F*) Basal metabolism, glycolytic capacity, glucose dependence, and AAO and FAO dependence of WT CD8$^+$ T cells stimulated for 17 h with anti-CD3/CD28 antibodies and rIL-2 were calculated according to the formula presented in *Materials and Methods*. (*G*) Basal metabolism of ex vivo KO or WT CD8$^+$ T cells or stimulated for 17 h or 48 h with anti-CD3/CD28 antibodies and rIL-2. n = 4 mice per group. (*H*) Glycolytic capacity of ex vivo KO or WT CD8$^+$ T cells or stimulated for 17 h or 48 h with anti-CD3/CD28 antibodies and rIL-2. n = 4 mice per group. $^{**}P < 0.01$. (*I*) Glucose dependence of ex vivo KO or WT CD8$^+$ T cells or stimulated for 17 h or 48 h with anti-CD3/CD28 antibodies and rIL-2. n = 4 mice per group. $^{**}P < 0.01$; $^{*}P < 0.05$. (*J*) Fatty acid (FA) and amino acid dependence of ex vivo KO or WT CD8$^+$ T cells or stimulated for 17 h or 48 h with anti-CD3/CD28 antibodies and rIL-2. n = 4 mice per group. $^{**}P < 0.01$.

indicated that lack of MCT1 expression did not temper the ability of T cells to produce ATP after stimulation. Remarkably, however, the higher global cellular energy charge observed in KO CD8$^+$ T cells appeared to be caused by reduced levels of nucleoside mono- and biphosphates in KO T cells, including IMP, AMP, ADP, CMP, CDP, GMP, GDP, UMP and UDP (Fig. 6 *F* and *I*). This reduction appeared to be transient, as indicated by analysis of the metabolome at a later time point (72 h) after stimulation (*SI Appendix*, Fig. S10). Taken together, these observations supported the idea that activated MCT1-deficient CD8$^+$ T cells maintain ATP at the expense of nucleotide synthesis and that limited glycolysis prevented cells from replenishing their nucleoside pools.

NAD$^+$ and NADP$^+$ levels detected by LC-MS were also strongly decreased in activated CD8$^+$ KO T cells (Fig. 6*J*). Direct quantification by a colorimetric assay highlighted the deficiency in total intracellular NAD (Fig. 6*K*). Nucleoside depletion has been shown to stimulate cell cycle arrest and DNA repair (47, 48), and NAD$^+$ is consumed by several enzymes involved in these processes such as sirtuins, which are NAD$^+$-dependent protein deacetylases, or poly

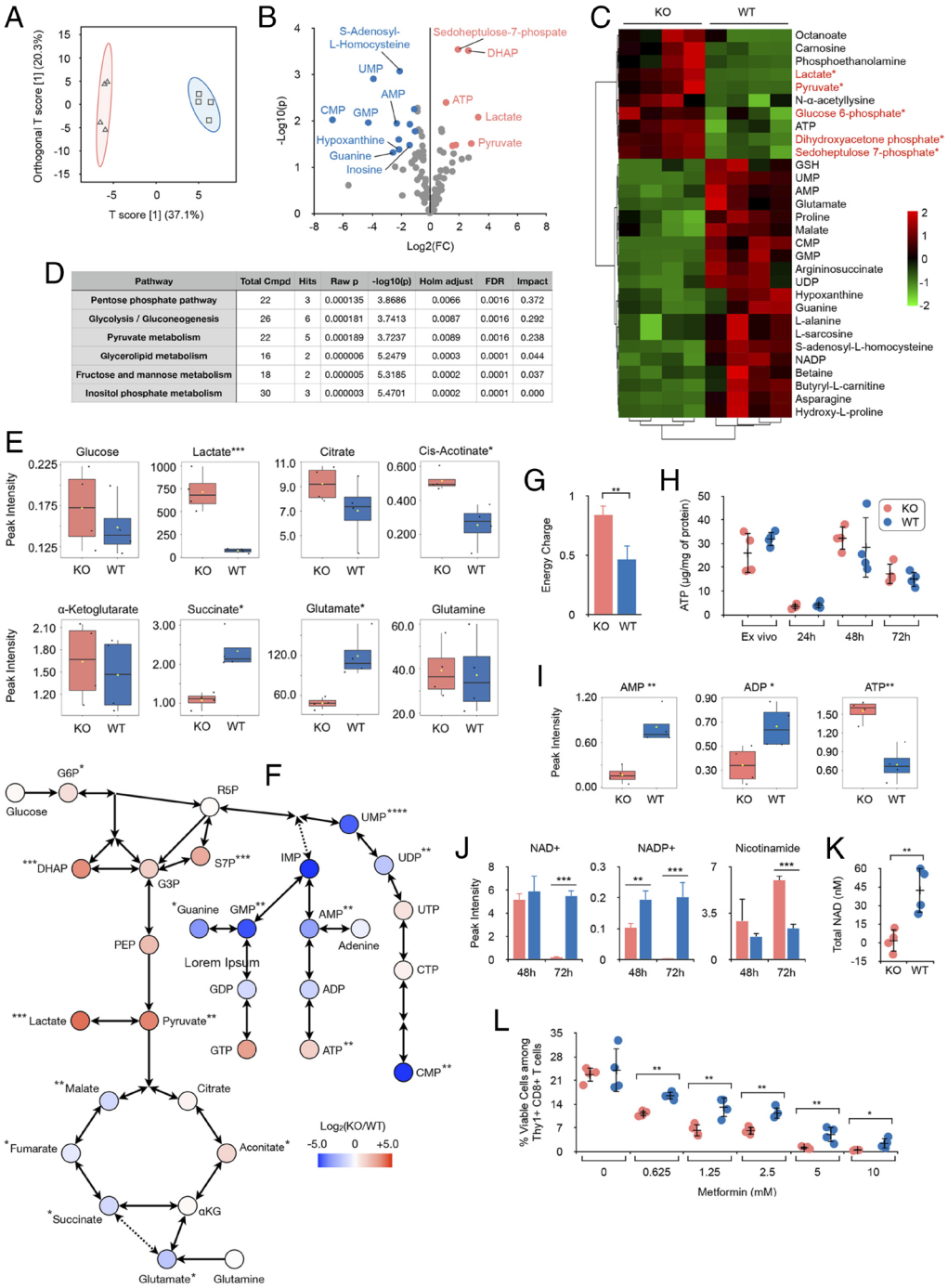

Fig. 6. Low level of glycolysis in activated MCT1-deficient CD8$^+$ T cells disrupts nucleotide synthesis and increases sensitivity to energy stress. (*A*) Partial least squares-discriminant analysis (PLS-DA). Cross-validated PLS-DA score plot for comparison of the global metabolite profiles (LC/MS-MS) of purified CD8$^+$ T cells from KO mice (n = 4 mice, △) and WT mice (n = 4 mice, 2) stimulated for 48 h with anti-CD3/CD28 antibodies and rIL-2. (*B*) Volcano plot of the differentially present metabolites (LC/MS-MS) in 48 h-stimulated KO and WT CD8$^+$ T cells. FC = fold changes (KO/WT). Red spots represent metabolites more present in purified CD8$^+$ T cells from KO mice (n = 4 mice); blue spots are metabolites more present in purified CD8$^+$ T cells from WT mice. (*C*) Two-way hierarchical clustering heatmap of metabolomic data (LC/MS-MS) for the 30 metabolites the most differentially present in 48-h activated KO and WT CD8$^+$ T cells. Each column shows the metabolic pattern of individual mice in the MCT1-deficient group (KO) and the control group (WT). Glycolysis intermediates are in red and indicated by an asterisk. (*D*) KEGG pathway analyses for the metabolites the most differentially present in 48-h activated KO and WT CD8$^+$ T cells. (*E*) Comparison of LC/MS-MS peak intensity of selected metabolites from glycolysis and TCA cycle isolated between 48-h activated KO and WT CD8$^+$ T cells. n = 4 mice per group. ***P < 0.001; **P < 0.01. (*F*) Log_2(KO/WT) analysis for targeted metabolites (LC/MS-MS) in glycolysis, TCA cycle, and nucleotide synthesis between 48-h-stimulated KO and WT CD8$^+$ T cells. (*G*) Energy charge in 48 h-stimulated KO and WT CD8$^+$ T cells was calculated according to the formula presented in *Materials and Methods*. n = 4 mice per group. **P < 0.01. (*H*) Amounts of ATP detected in KO and WT CD8$^+$ T cells, ex vivo or stimulated for the indicated times with anti-CD3/CD28 antibodies and recombinant IL-2. n = 4 mice per group. (*I*) Comparison of LC/MS-MS peak intensity of AMP, ADP et ATP between 48-h activated KO and WT CD8$^+$ T cells. n = 4 mice per group. **P < 0.01; *P < 0.05. (*J*) Comparison of LC/MS-MS peak intensity of NAD$^+$, NADP$^+$, and nicotinamide between 48-h- and 72-h activated KO and WT CD8$^+$ T cells. n = 4 mice per group. ***P < 0.001; **P < 0.01. (*K*) Total NAD quantified in 72-h activated KO and WT CD8$^+$ T cells. n = 4 mice per group. **P < 0.01. (*L*) Percent of viable KO and WT CD8$^+$ T cells stimulated for 72 h with anti-CD3/CD28 antibodies and rIL-2 in the presence of metformin. n = 4 mice per group. **P < 0.01; *P < 0.05.

(ADP-ribose) polymerases (PARP), which consume NAD^+ for the synthesis of poly(ADP-ribose) (49, 50). Extensive NAD^+ consumption was also supported by the accumulation of nicotinamide in activated MCT1-deficient $CD8^+$ T cells (Fig. 6*J*). Therefore, we reasoned that if KO T cells were limited in their capacity to maintain NAD levels, they should be more sensitive to energy stress induced by pharmacological inhibition of mitochondrial complex I. As displayed in Fig. 6*L*, T cell viability decreased in cultures of WT T cells containing metformin, known to inhibit complex I of the respiratory chain (51). Remarkably, metformin-induced cell death was significantly increased in activated KO $CD8^+$ T cells, which was expected since NAD abundance was limited in these cells (Fig. 6*L*).

Discussion

The main observation reported here is that expression of the lactate transporter MCT1 is required for T cell proliferation induced by antigen recognition. It is also shown that limited antigen-driven expansion prevents virus-specific MCT1-deficient $CD8^+$ T cells to ensure protective immunity toward acute viral infection. More importantly, our results demonstrate the critical importance of MCT1 for the control of viral replication by T cells and the selection of the mechanism responsible for maintaining persistent MuHV-4 infection. It is well known that the dose of virus to which virus-specific $CD8^+$ T cells are exposed determines whether this leads to normal function, reversible functional exhaustion, or terminal exhaustion in T cells (13). Our results show that increased viral replication caused by the failure of MCT1-deficient T cells to expand following activation creates the necessary conditions for the induction of functional exhaustion among MuHV-4-specific $CD8^+$ T cells. Conversely, they demonstrate that a competent immune control of infection is required for the maintenance of long-term viral latency. In light of this, we can consider several scenarios that might explain the differences in T cell functionality that lead to either chronic virus replication or viral latency. From the initial work of several groups, we know that the initial stage of MuHV-4 replication in lung epithelial cells is controlled by cytotoxic $CD8^+$ T cells (52, 53). It is also known from experimental evidence that the abundance and availability of viral antigen defines the extent of T cell exhaustion (17). Failure to limit viral replication by MCT1-deficient $CD8^+$ T cells increases the amount of antigens available to stimulate T cells and thus induces functional exhaustion. Immune exhaustion is typically set up by RNA virus infections, where IFN-dependent silencing of DNA transcription cannot limit antigen expression (54). Rapid replication leading to functional exhaustion is then achieved to evade cytotoxic T cells and establish chronic infection. Since, in our study, MCT1-deficient MuHV-4-specific $CD8^+$ Tex cells displayed a deficit in IFNγ production, it is reasonable to assume that IFN-dependent antigen transcriptional repression is decreased in MuHV-4-infected KO mice, preventing the induction of viral latency but maintaining T cell exhaustion. Thus, our study shows that MuHV-4 infection in mice whose T cells are deficient for MCT1 offers a unique model for comparing the mechanisms responsible for persistent viral latency or chronic infection leading to functional exhaustion of virus-specific $CD8^+$ T cells.

Unlike what was observed for MuHV-4 infection, the inability of MCT1-deficient $CD8^+$ T lymphocytes to control PVM infection did not lead to chronic infection characterized by the persistence of virus-specific exhausted $CD8^+$ T cells. Although T cells are known to have no apparent impact on the outcome of acute lethal PVM infection, both $CD4^+$ and $CD8^+$ T cells are required for virus clearance in response to sublethal PVM infection (30). The observation made by others that pulmonary PVM-specific $CD8^+$ T cells displayed a deficit in their capacity to produce proinflammatory cytokines such as IFNγ has suggested that PVM may severely impair the functionality of $CD8^+$ effector T cells (55). Our results indicate that limited expansion of MCT1-deficient $CD8^+$ T cells could add to the capacity of PMV to inhibit T cell effector function as shown by their poorer ability to produce IFNγ than WT $CD8^+$ T cells. The molecular mechanism used by PVM to inhibit the function $CD8^+$ T cells remains elusive. Whether it involves the induction of functional exhaustion among T cells is unknown.

We also report that MCT1 is required for optimal glycolytic activity in dividing T cells. Moreover, while reduced glycolysis is observed in activated MCT1-deficient T cells, this situation does not lead to cellular energy depletion. We observed, however, that lack of MCT1 expression leads to the depletion of mono- and diphosphate nucleosides and subsequently renders T cells more susceptible to energy stress. The synthesis of purine and pyrimidine nucleotides is necessary for T cell proliferation, but each regulates the cell cycle differently. Purines were shown to control both the transition from G(1) to S phase and progression through S phase, while pyrimidines would only control progression from early to middle S phase (56). Interestingly, the alteration of T lymphocyte glycolytic activity linked to inhibition of proliferation by PD1 checkpoint was recently shown to involve a block of de novo nucleoside phosphate synthesis (48). These results confirm that limited nucleotide synthesis is a consequence of glycolysis inhibition in activated T cells. Though this situation certainly impacts T cell proliferation, it appears to have a limited effect on cellular energy homeostasis, since normal levels of NTPs, and ATP in particular, were found in activated MCT1-deficient $CD8^+$ T cells. Thus, a limited glycolytic activity coupled to the need to maintain cellular energy causes the specific depletion of mono- and diphosphate nucleosides. This conclusion is also supported by the observation that the partial restoration of glycolysis in MCT1-deficient T cells, which correlates with the late increase in MCT4 expression, appears to restore the production of nucleosides.

As mentioned earlier, MCT1-mediated lactate transport in T cells appears to depend directly on the difference in concentration of lactate on either side of the cell plasma membrane. Recently, MCT1 was shown to be responsible for lactate intake and oxidation by Tregs in low-glucose/high-lactate environment such as solid tumors (23, 24). Moreover, MCT1 and downstream lactate signaling in Tregs can confer resistance to anti-PD1 therapy and would be a marker of poor prognosis in hepatocellular carcinoma (57). Initial experimental studies, however, described MCT1 as an indispensable transporter for the extraction of lactate from human activated T lymphocytes, pharmacological inhibition of MCT1 activity limiting cell proliferation (22). Likewise, a recent study by Macchi et al. (27) confirmed our observation that targeted silencing of MCT1 limited $CD8^+$ T cell proliferation while it had little impact on that of $CD4^+$ T cells. Although this study reached the same conclusions as our study on the importance of lactate extraction by MCT1 for the proliferation of $CD8^+$ T cells, major differences were observed regarding the metabolic consequences of MCT1 deficiency. While just like us glycolysis inhibition and compensation by increased oxidative phosphorylation were observed by Macchi et al. in activated MCT1-deficient $CD8^+$ T cells, the accumulation of glycolytic intermediates, however, was not seen. This discrepancy may be due to the different experimental protocols used in the two studies. Whereas we focused our attention more specifically on the early stages of T cell activation (48 h after activation), Macchi and his colleagues only analyzed the changes observed later (96 h), at time points where MCT4 is

presumed to play a major role in lactate extraction. This could explain why accumulation of glycolytic metabolites was not observed in their study.

MCTs are important for cancer cell proliferation, survival, and metastasis. Specific MCT1 inhibitors have been developed as potential antitumor agents, and one of them (AZD3965) is in phase I clinical trials for advanced cancers (58). In this context, our results indicate that a therapy based on the inhibition of MCT1 could have deleterious effects on the generation of antitumor immunity. On the contrary, our findings open up opportunities to better understand how T cell metabolism is at the heart of immune responses and could therefore be the target for the development of therapies, especially in immunopathologies where an exacerbated T cell response causes the disease.

Materials and Methods

Additional methods are provided in *SI Appendix*.

Briefly, mouse T cells were made deficient for MCT1 expression by crossing B6.Slc16a1fl/fl mice with B6.CD4Cre mice. Proliferative capacity and energy metabolism of MCT1-deficient T cells were analyzed after activation with immobilized anti-CD3 and soluble anti-CD28. rIL-2 was also added to CD8+ T cell cultures. MCT1-deficient T cells were analyzed in vivo for their capacity to respond to infection with pneumonia virus of mice (PVM) or gamma herpesvirus MuHV-4.

Data, Materials, and Software Availability. All study data are included in the article and/or *SI Appendix*.

ACKNOWLEDGMENTS. This work was supported by the Belgian Fonds de la Recherche Scientifique-Fonds National de la Recherche Scientifique (FRS-FNRS), the Télévie, the European Union (EU) FEDER program, the European Research Council (ERC) independent researcher starting grant (TUMETABO) as well as by the ERC Starting Grant (to B.M.) (ERC-StG-2019 VIROME, ID853608) and by the FRS-FNRS under the Excellence of Science (EOS) program (grant ID 40007527). S.L. is supported by the Chinese Scholarship Council (CSC). S. D'Aria, M.F., and V.F.V.H. are Télévie Fellows. C.M. is a Research Fellow, B.M. a Research Associate, and P.S. is a Research Director of the FRS-FNRS.

Author affiliations: [a]Institute for Medical Immunology, Faculty of Medicine, Université libre de Bruxelles, Gosselies 6041, Belgium; [b]Immunology-Vaccinology, Department of Infectious and Parasitic Diseases, Faculty of Veterinary Medicine - Fundamental and Applied Research for Animals & Health Research Unit, University of Liège, Liège 4000, Belgium; [c]Pole of Pharmacology, Institut de Recherche Expérimentale et Clinique, Université catholique de Louvain, Brussels 1200, Belgium; [d]Immunobiology Laboratory, Faculty of Sciences, Université libre de Bruxelles, Gosselies 6041, Belgium; [e]Plateforme d'étude du métabolisme, Institut Necker, Inserm US 24 - CNRS UMS 3633, Faculté de Médecine Paris Descartes, Paris 75015, France; and [f]WEL Research Institute, Welbio Department, Wavre 1300, Belgium

1. D. L. Barber *et al.*, Restoring function in exhausted CD8 T cells during chronic viral infection. *Nature* **439**, 682–687 (2006).
2. J. C. Beltra *et al.*, Developmental relationships of four exhausted CD8(+) T cell subsets reveals underlying transcriptional and epigenetic landscape control mechanisms. *Immunity* **52**, 825–841. e828 (2020).
3. B. Bengsch *et al.*, Bioenergetic insufficiencies due to metabolic alterations regulated by the inhibitory receptor PD-1 are an early driver of CD8(+) T cell exhaustion. *Immunity* **45**, 358–373 (2016).
4. M. Bettonville *et al.*, Long-term antigen exposure irreversibly modifies metabolic requirements for T cell function. *Elife* **7**, e30938 (2018).
5. W. H. Hudson *et al.*, Proliferating transitory T cells with an effector-like transcriptional signature emerge from PD-1(+) stem-like CD8(+) T cells during chronic infection. *Immunity* **51**, 1043–1058. e1044 (2019).
6. P. J. Farrell, Epstein-Barr virus and cancer. *Annu. Rev. Pathol.* **14**, 29–53 (2019).
7. P. G. Stevenson, Immune control of γ-herpesviruses. *Viral Immunol.* **33**, 225–232 (2020).
8. N. Zangger, A. Oxenius, T cell immunity to cytomegalovirus infection. *Curr. Opin. Immunol.* **77**, 102185 (2022).
9. B. Polić *et al.*, Hierarchical and redundant lymphocyte subset control precludes cytomegalovirus replication during latent infection. *J. Exp. Med.* **188**, 1047–1054 (1998).
10. A. Hoji *et al.*, Early KLRG1(+) but not CD57(+)CD8(+) T cells in primary cytomegalovirus infection predict effector function and viral control. *J. Immunol.* **203**, 2063–2075 (2019).
11. A. Lang, J. Nikolich-Zugich, Functional CD8 T cell memory responding to persistent latent infection is maintained for life. *J. Immunol.* **187**, 3759–3768 (2011).
12. C. M. Snyder *et al.*, Memory inflation during chronic viral infection is maintained by continuous production of short-lived, functional T cells. *Immunity* **29**, 650–659 (2008).
13. D. Moskophidis, F. Lechner, H. Pircher, R. M. Zinkernagel, Virus persistence in acutely infected immunocompetent mice by exhaustion of antiviral cytotoxic effector T cells. *Nature* **362**, 758–761 (1993).
14. M. F. Callan *et al.*, Large clonal expansions of CD8+ T cells in acute infectious mononucleosis. *Nat. Med.* **2**, 906–911 (1996).
15. M. F. Callan *et al.*, Direct visualization of antigen-specific CD8+ T cells during the primary immune response to Epstein-Barr virus In vivo. *J. Exp. Med.* **187**, 1395–1402 (1998).
16. P. G. Stevenson, G. T. Belz, J. D. Altman, P. C. Doherty, Changing patterns of dominance in the CD8+ T cell response during acute and persistent murine gamma-herpesvirus infection. *Eur J. Immunol.* **29**, 1059–1067 (1999).
17. A. Bergthaler *et al.*, Viral replicative capacity is the primary determinant of lymphocytic choriomeningitis virus persistence and immunosuppression. *Proc. Natl. Acad. Sci. U.S.A.* **107**, 21641–21646 (2010).
18. H. Shin, S. D. Blackburn, J. N. Blattman, E. J. Wherry, Viral antigen and extensive division maintain virus-specific CD8 T cells during chronic infection. *J. Exp. Med.* **204**, 941–949 (2007).
19. E. J. Usherwood *et al.*, Control of gammaherpesvirus latency by latent antigen-specific CD8(+) T cells. *J. Exp. Med.* **192**, 943–952 (2000).
20. R. Wang *et al.*, The transcription factor Myc controls metabolic reprogramming upon T lymphocyte activation. *Immunity* **35**, 871–882 (2011).
21. J. Pérez-Escuredo *et al.*, Monocarboxylate transporters in the brain and in cancer. *Biochim. Biophys. Acta* **1863**, 2481–2497 (2016).
22. C. M. Murray *et al.*, Monocarboxylate transporter MCT1 is a target for immunosuppression. *Nat. Chem. Biol.* **1**, 371–376 (2005).
23. M. J. Watson *et al.*, Metabolic support of tumour-infiltrating regulatory T cells by lactic acid. *Nature* **591**, 645–651 (2021).
24. S. Kumagai *et al.*, Lactic acid promotes PD-1 expression in regulatory T cells in highly glycolytic tumor microenvironments. *Cancer Cell* **40**, 201–218.e209 (2022).
25. I. Kaymak *et al.*, Carbon source availability drives nutrient utilization in CD8(+) T cells. *Cell Metab.* **34**, 1298–1311.e1296 (2022).
26. A. J. M. Howden *et al.*, Quantitative analysis of T cell proteomes and environmental sensors during T cell differentiation. *Nat. Immunol.* **20**, 1542–1554 (2019).
27. C. Macchi *et al.*, Monocarboxylate transporter 1 deficiency impacts CD8(+) T lymphocytes proliferation and recruitment to adipose tissue during obesity. *iScience* **25**, 104435 (2022).
28. H. W. Virgin, E. J. Wherry, R. Ahmed, Redefining chronic viral infection. *Cell* **138**, 30–50 (2009).
29. M. J. Cannon, P. J. Openshaw, B. A. Askonas, Cytotoxic T cells clear virus but augment lung pathology in mice infected with respiratory syncytial virus. *J. Exp. Med.* **168**, 1163–1168 (1988).
30. S. Frey, C. D. Krempl, A. Schmitt-Gräff, S. Ehl, Role of T cells in virus control and disease after infection with pneumonia virus of mice. *J. Virol.* **82**, 11619–11627 (2008).
31. K. B. Walsh *et al.*, CD8+ T-cell epitope mapping for pneumonia virus of mice in H-2b mice. *J. Virol.* **87**, 9949–9952 (2013).
32. P. G. Stevenson, R. D. Cardin, J. P. Christensen, P. C. Doherty, Immunological control of a murine gammaherpesvirus independent of CD8+ T cells. *J. Gen. Virol.* **80**, 477–483 (1999).
33. S. François *et al.*, Comparative study of murid gammaherpesvirus 4 infection in mice and in a natural host, bank voles. *J. Gen. Virol.* **91**, 2553–2563 (2010).
34. R. Milho *et al.*, In vivo imaging of murid herpesvirus-4 infection. *J. Gen. Virol.* **90**, 21–32 (2009).
35. H. T. Jin *et al.*, Cooperation of Tim-3 and PD-1 in CD8 T-cell exhaustion during chronic viral infection. *Proc. Natl. Acad. Sci. U.S.A.* **107**, 14733–14738 (2010).
36. F. Alfei *et al.*, TOX reinforces the phenotype and longevity of exhausted T cells in chronic viral infection. *Nature* **571**, 265–269 (2019).
37. O. Khan *et al.*, TOX transcriptionally and epigenetically programs CD8(+) T cell exhaustion. *Nature* **571**, 211–218 (2019).
38. H. Seo *et al.*, TOX and TOX2 transcription factors cooperate with NR4A transcription factors to impose CD8(+) T cell exhaustion. *Proc. Natl. Acad. Sci. U.S.A.* **116**, 12410–12415 (2019).
39. N. B. Beyersdorf, X. Ding, K. Karp, T. Hanke, Expression of inhibitory "killer cell lectin-like receptor G1" identifies unique subpopulations of effector and memory CD8 T cells. *Eur J. Immunol.* **31**, 3443–3452 (2001).
40. R. J. Argüello *et al.*, SCENITH: A flow cytometry-based method to functionally profile energy metabolism with single-cell resolution. *Cell Metab.* **32**, 1063–1075.e1067 (2020).
41. J. R. Doherty *et al.*, Blocking lactate export by inhibiting the Myc target MCT1 Disables glycolysis and glutathione synthesis. *Cancer Res.* **74**, 908–920 (2014).
42. R. A. Noble *et al.*, Inhibition of monocarboxyate transporter 1 by AZD3965 as a novel therapeutic approach for diffuse large B-cell lymphoma and Burkitt lymphoma. *Haematologica* **102**, 1247–1257 (2017).
43. K. A. Frauwirth *et al.*, The CD28 signaling pathway regulates glucose metabolism. *Immunity* **16**, 769–777 (2002).
44. S. Kang *et al.*, GAB functions as a bioenergetic and signalling gatekeeper to control T cell inflammation. *Nat. Metab.* **4**, 1322–1335 (2022).
45. J. G. McCormack, R. M. Denton, The effects of calcium ions and adenine nucleotides on the activity of pig heart 2-oxoglutarate dehydrogenase complex. *BioChem J.* **180**, 533–544 (1979).
46. V. B. Lawlis, T. E. Roche, Inhibition of bovine kidney alpha-ketoglutarate dehydrogenase complex by reduced nicotinamide adenine dinucleotide in the presence or absence of calcium ion and effect of adenosine 5′-diphosphate on reduced nicotinamide adenine dinucleotide inhibition. *Biochemistry* **20**, 2519–2524 (1981).
47. K. Hastak *et al.*, DNA synthesis from unbalanced nucleotide pools causes limited DNA damage that triggers ATR-CHK1-dependent p53 activation. *Proc. Natl. Acad. Sci. U.S.A.* **105**, 6314–6319 (2008).
48. N. J. Palaskas *et al.*, Global alteration of T-lymphocyte metabolism by PD-L1 checkpoint involves a block of de novo nucleoside phosphate synthesis. *Cell Discov.* **5**, 62 (2019).
49. W. Gu, R. G. Roeder, Activation of p53 sequence-specific DNA binding by acetylation of the p53 C-terminal domain. *Cell* **90**, 595–606 (1997).

50. L. Qiang *et al.*, Brown remodeling of white adipose tissue by SirT1-dependent deacetylation of Pparγ. *Cell* **150**, 620–632 (2012).
51. W. W. Wheaton *et al.*, Metformin inhibits mitochondrial complex I of cancer cells to reduce tumorigenesis. *Elife* **3**, e02242 (2014).
52. S. Ehtisham, N. P. Sunil-Chandra, A. A. Nash, Pathogenesis of murine gammaherpesvirus infection in mice deficient in CD4 and CD8 T cells. *J. Virol.* **67**, 5247–5252 (1993).
53. D. J. Topham *et al.*, Perforin and Fas in murine gammaherpesvirus-specific CD8(+) T cell control and morbidity. *J. Gen. Virol.* **82**, 1971–1981 (2001).
54. L. Cicin-Sain, R. Arens, Exhaustion and inflation at antipodes of T cell responses to chronic virus infection. *Trends Microbiol.* **26**, 498–509 (2018).
55. E. A. Claassen *et al.*, Activation and inactivation of antiviral CD8 T cell responses during murine pneumovirus infection. *J. Immunol.* **175**, 6597–6604 (2005).
56. L. Quéméneur *et al.*, Differential control of cell cycle, proliferation, and survival of primary T lymphocytes by purine and pyrimidine nucleotides. *J. Immunol.* **170**, 4986–4995 (2003).
57. J. Zhou *et al.*, Monocarboxylate transporter upregulation in induced regulatory T cells promotes resistance to anti-PD-1 therapy in hepatocellular carcinoma patients. *Front Oncol.* **12**, 960066 (2022).
58. M. Beloueche-Babari *et al.*, MCT1 inhibitor AZD3965 increases mitochondrial metabolism, facilitating combination therapy and noninvasive magnetic resonance spectroscopy. *Cancer Res.* **77**, 5913–5924 (2017).